Acta Crystallographica Section D
Biological Crystallography
ISSN 0907-4449

Structure of 2-haloacid dehalogenase from *Pseudomonas syringae* pv. *tomato* DC3000

Zhiqiang Hou,[a,b]‡ Hongmei Zhang,[a]‡ Mei Li[a]* and Wenrui Chang[a]*

[a]National Laboratory of Biomacromolecules, Institute of Biophysics, Chinese Academy of Sciences, 15 Datun Road, Chaoyang District, Beijing 100101, People's Republic of China, and [b]University of the Chinese Academy of Sciences, Beijing 100049, People's Republic of China

‡ These authors contributed equally to this work.

Correspondence e-mail: meili@moon.ibp.ac.cn, wrchang@sun5.ibp.ac.cn

Received 2 November 2012
Accepted 3 March 2013

PDB Reference: ps-2-HAD, 3vay

2-Haloacid dehalogenases (2-HADs) catalyse the hydrolytic dehalogenation of 2-haloalkanoic acids, cleaving the carbon–halide bond at the C^{α}-atom position and releasing a halogen atom. These enzymes are of interest for their potential use in bioremediation and in the synthesis of industrial chemicals. Here, the crystal structure of 2-HAD from *Pseudomonas syringae* pv. *tomato* DC3000 (ps-2-HAD) at 1.98 Å resolution solved using the single-wavelength anomalous dispersion method is reported. The ps-2-HAD molecule consists of two structurally distinct domains: the core domain and the subdomain. Enzymatic activity analysis of ps-2-HAD revealed its capacity to catalyse the dehalogenation of both L- and D-substrates; however, the structure of ps-2-HAD is completely different from that of DehI, which is the only DL-2-HAD enzyme that has been structurally characterized, but shows similar overall folding to L-HADs. Single mutations of four amino-acid residues at the putative active site showed that they are related to its enzymatic activity, yet three of them are nonconserved among HADs. These observations imply that ps-2-HAD has a novel active site and a unique catalytic behaviour compared with other HADs. This study provides a structural basis and biochemical evidence for further elucidation of the catalytic mechanism of 2-HAD.

1. Introduction

Halogenated organic compounds are widely used in the industrial-scale manufacture of herbicides, pesticides and industrial solvents. Halogen substitution causes serious environmental problems as it increases toxicity and recalcitrance to degradation. Dehalogenases can be used to degrade halogenated environmental pollutants and thus have been the target of bioremedial research (Schmidberger *et al.*, 2008).

2-Haloacid dehalogenases (2-HADs) catalyse the hydrolytic dehalogenation of 2-haloalkanoic acids at the C^{α}-atom position with the release of a halogen atom. The reaction is

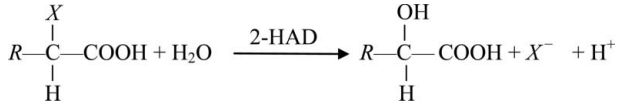

where *R* is H or an alkyl group (typically fewer than three C atoms) and *X* is a halide atom (Cl or Br) (Liu *et al.*, 1994). Based on their substrate specificities and the configurations of their products, 2-HADs are classified into three types. DL-2-HADs catalyse the dehalogenation of both D- and L-2-haloalkanoic acids, inverting the stereochemistry at the C^{α}-atom position and producing the corresponding L- and

© 2013 International Union of Crystallography
Printed in Singapore – all rights reserved

D-products, respectively. D- and L-2-HADs act specifically on only one enantiomer and cause inversion of C^{α}-atom stereochemistry in the hydroxyalkanoic acid product (Littlechild *et al.*, 2009; Hisano *et al.*, 1996).

L-2-HADs have been better characterized both biochemically and structurally. There are currently four structures available: those of L-DEX YL from *Pseudomonas* sp. YL (Hisano *et al.*, 1996), DhlB from *Xanthobacter autotrophicus* GJ10 (Ridder *et al.*, 1997), DehIVa from *Burkholderia cepacia* MBA4 (Schmidberger *et al.*, 2007) and L-haloacid dehalogenase from the thermophilic archaeon *Sulfolobus tokodaii* (Littlechild *et al.*, 2009). These structures are similar, with each molecule consisting of a core domain and a subdomain, while DhlB has an additional dimerization domain comprised of two antiparallel α-helices (Ridder *et al.*, 1997). In substrate–enzyme cocrystal structures such as those of L-DEX YL (PDB entries 1zrm and 1zrn; Li *et al.*, 1998), DhlB (PDB entries 1qq6 and 1qq7; Ridder *et al.*, 1999) and DehIVa (PDB entry 2no5; Schmidberger *et al.*, 2007), the enzyme covalently bound to a substrate with an extremely conserved Asp residue has been trapped as a reaction intermediate. These structures and the biochemical results of Liu *et al.* (1994) show that the reaction mechanism of L-2-HADs involves a two-step nucleophilic attack: firstly, the most conserved Asp residue in the catalytic site acts at the C^{α} atom of the substrate to form an esterified intermediate and, secondly, an activated water molecule attacks the carboxyl C atom of the Asp to cleave the ester bond. In a mutagenesis experiment using L-DEX YL, the enzyme activity was completely lost when the conserved aspartate (Asp10) was mutated (Liu *et al.*, 1994, 1997; Kurihara *et al.*, 1995).

Compared with the L-2-HADs, little is known about the structure and reaction mechanisms of the D- and DL-2-HADs. To date, no crystal structures and few functional investigations of D-2-HADs have been reported. Only one crystal structure of a DL-2-HAD, that of DehI from *P. putida* strain PP3, has been reported (Schmidberger *et al.*, 2008). The three-dimensional structure of DehI folds in a totally different manner from those of L-2-HADs. D-2-HADs and DL-2-HADs share approximately 20% sequence homology, and are both markedly different from the L-2-HADs. In addition, the conserved aspartate residue in L-2-HADs is missing in D- and DL-HADs (Nardi-Dei *et al.*, 1997). These results indicate that DL-2-HADs may adopt a different catalytic mechanism from L-2-HADs. Esaki and coworkers determined the reaction mechanism of another DL-2-HAD (DL-DEX 113) by means of ^{18}O-incorporation experiments (Esaki *et al.*, 1999) and found that the reaction does not involve the formation of an ester intermediate. They hypothesized that the carbon–halide bond in DL-2-HADs may be cleaved by an activated water molecule directly attacking the C^{α} atom of D- and DL-2-haloalkanoic acids to displace the halogen atom.

To obtain further insight into the reaction mechanism of 2-HADs, we solved the crystal structure of ps-2-HAD from *P. syringae* pv. *tomato* DC3000 at 1.98 Å resolution. Analysis of the activity of ps-2-HAD revealed its capacity to catalyse the dehalogenation of both L- and D-substrates. However, a structural comparison showed that the structure of ps-2-HAD is similar overall to those of L-2-HADs, but is significantly different from that of DehI. We also found that the activity of ps-2-HAD is suppressed by Mg^{2+}. Several mutants of ps-2-HAD were constructed in order to identify the critical amino-acid residues that are important for enzymatic activity. The functional mechanism of ps-2-HAD is discussed based on the crystal structure, analysis of the enzyme activity and mutation information.

Table 1
Data-collection and structure-refinement statistics for ps-2-HAD.

Values in parentheses are for the highest resolution shell.

	Native	Iodide derivative
Data collection		
Wavelength (Å)	0.98	1.7
Space group	$P2_1$	$P2_1$
Unit-cell parameters (Å, °)	a = 44.0, b = 91.0, c = 69.8, β = 108.3	a = 44.3, b = 92.3, c = 70.2, β = 108.1
No. of molecules in asymmetric unit	2	2
Solvent content	0.54	0.55
Resolution range (Å)	50–2.00	50–1.98
Unique reflections	33928	35295
Multiplicity	7.0 (7.1)	14.6 (14.7)
Completeness (%)	95.2 (93.0)	94.4 (90.7)
R_{merge} (%)	8.2 (59.9)	9.0 (45.4)
Refinement statistics		
Resolution range (Å)		25–1.98
R_{work} (%)		19.3
R_{free} (%)		22.4
No. of protein atoms		3622
No. of water molecules		334
R.m.s.d., bond lengths (Å)		0.008
R.m.s.d., bond angles (°)		1.105
Average B factor (Å^2)		29.7
Ramachandran statistics, residues in (%)		
Most favoured regions		91.3
Allowed regions		8.7

2. Materials and methods

2.1. Cloning, expression and purification

The *pspto_0221* gene encoding ps-2-HAD was amplified by PCR from *P. syringae* pv. *tomato* DC3000 genomic DNA, cloned into PGEX-6P-1 vector and expressed in *Escherichia coli* strain BL21 (DE3) (Novagen) with an N-terminal glutathione *S*-transferase (GST) tag. The cells were harvested by centrifugation, resuspended in PBS buffer (10 m*M* Na_2HPO_4 pH 7.3, 1.8 m*M* KH_2PO_4, 140 m*M* NaCl, 2.7 m*M* KCl) and sonicated for 20 min. The protein was purified by passage through two GST affinity columns, with PreScission protease cleavage on the first column overnight in cleavage buffer [50 m*M* Tris–HCl pH 7.5, 150 m*M* NaCl, 1 m*M* ethylenediamine tetraacetic acid (EDTA), 1 m*M* dithiothreitol]. Samples were concentrated to 9 mg ml^{-1} in Tris buffer (50 m*M* Tris pH 8.0, 25 m*M* NaCl) for crystallization and phenol red enzyme assays or in HEPES buffer [100 m*M* hydroxylethyl-1-piperazineethanesulfonic acid (HEPES) pH 8.2] for mercuric thiocyanate enzyme assays.

2.2. Crystallization and data collection

Crystals of ps-2-HAD were grown using the sitting-drop vapour-diffusion method. A drop of protein solution mixed with an equal volume of reservoir solution consisting of 0.2 *M* $MgCl_2.6H_2O$, 20–26% PEG 4K, 0.1 *M* Tris pH 8.5 was equilibrated against 100 µl reservoir solution. Crystals of good diffraction quality were obtained overnight at 277 K. After soaking in reservoir solution to which 1.25 *M* KI had been added, the crystal was flash-cooled in a nitrogen-gas stream at 100 K for data collection. Diffraction data for the heavy-atom derivative of ps-2-HAD were collected on BL17U at Shanghai Synchrotron Radiation Facility. The diffraction data were processed and scaled with *HKL*-2000 (Otwinowski & Minor, 1997).

2.3. Structure determination and refinement

The single-wavelength anomalous dispersion method was used to solve the structure of ps-2-HAD. The initial phase was obtained using *AutoSol* from the *PHENIX* suite (Adams *et al.*, 2010) and was further improved by density modification with *RESOLVE* (Terwilliger, 2000), which increased the FOM from 0.33 to 0.69. *AutoBuild* from the *PHENIX* suite was used to build 81% of the main chain of ps-2-HAD and the remaining residues were rebuilt manually by *Coot* (Emsley & Cowtan, 2004). The model was refined using *phenix.refine* and *REFMAC*5 (Winn *et al.*, 2011). The stereochemical quality of the final model was checked with *PROCHECK* (Laskowski *et al.*, 1993). Structural figures were prepared using *PyMOL* (http://www.pymol.org). A summary of the data-collection and structure-refinement statistics is given in Table 1. The atomic coordinates of the ps-2-HAD crystal structure have been deposited in the Protein Data Bank as entry 3vay.

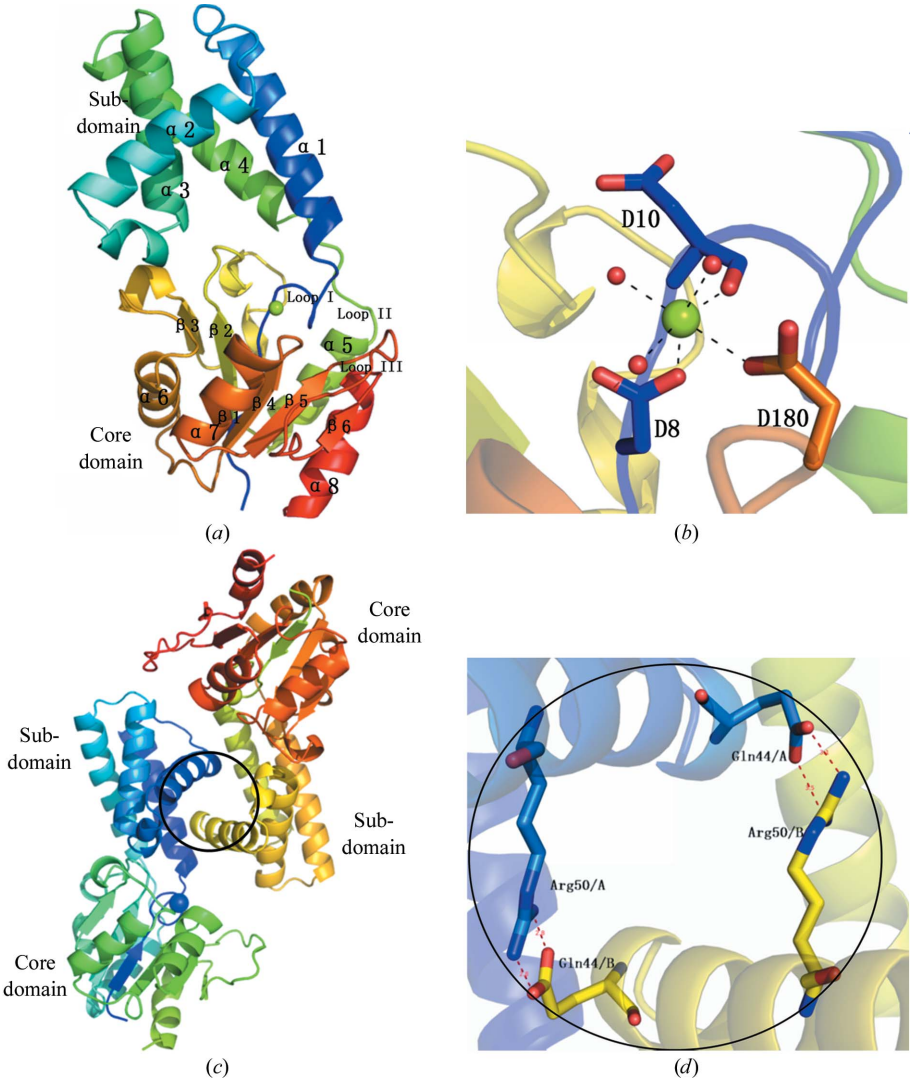

Figure 1
(*a*) Ribbon representation of the ps-2-HAD monomer with different structural elements labelled and magnesium shown as a green ball. (*b*) Magnesium coordination. The Mg atom is shown as a green ball; three water molecules are shown as small red balls and three ligated Asp residues are shown as sticks. Hydrogen bonds are shown as black dashed lines. (*c*) Interaction between two ps-2-HAD molecules in an asymmetric unit. Both molecules are shown as rainbow-coloured models. Interactions between the two molecules are shown in a black circle. (*d*) Molecule *A* (blue) and molecule *B* (yellow) interact with each other *via* hydrogen bonds (red dashed lines). Residues that form hydrogen bonds are shown as sticks.

2.4. Activity assay

A colorimetric enzyme assay based on the method of Littlechild *et al.* (2009) was performed with minor modifications. Briefly, the total reaction volume of 100 µl was made up of 1 m*M* HEPES pH 8.2, 15 m*M* Na_2SO_4, 1 m*M* EDTA, 20 µg ml^{-1} phenol red solution and 10 m*M* substrate. After incubation at room temperature for 5 min, 2 µl purified ps-2-HAD (18 µg) was added and activity was detected by measuring the decrease in absorbance at 540 nm. All absorption values were inverted for ease of analysis. Enzyme activity was measured as the initial reaction velocity over 5 s.

The activity of ps-2-HAD towards D- and L-2-substrates was also assayed by measuring chloride-ion release (modified from Iwasaki, Kokubu *et al.*, 1956). The standard assay-system volume of 150 µl was made up of 1 m*M* HEPES pH 8.2, 15 m*M* Na_2SO_4, 200 m*M* L- or D-2-CPA and the amounts of enzyme indicated. After incubation at room temperature for 15 min, the reaction was terminated by the addition of 16.65 µl 1.5 *M* sulfuric acid. The chloride ions released were determined spectrophotometrically at 460 nm after adding 66 µl ferric ammonium sulfate (made by dissolving 8 g ferric ammonium sulfate in 100 ml 6 *M* nitric acid) and 198 µl mercuric thiocyanate (made by dissolving 100 mg mercuric

thiocyanate in 100 ml of a mixed solvent consisting of nine volumes of dioxane and one volume of alcohol).

3. Results and discussion

3.1. Overall structure of ps-2-HAD

The final model of ps-2-HAD consists of two molecules (*A* and *B*) in the asymmetric unit. All 230 amino-acid residues were traced in each molecule. The loop regions of ps-2-HAD fitted the electron density well. Each monomer has approximate dimensions of 62 × 27 × 25 Å (Fig. 1).

The ps-2-HAD molecule consists of two domains referred to as the core domain and the subdomain (Fig. 1*a*). The core domain includes residues 1–7 and 110–230, which represent approximately 56% of the amino-acid residues of the protein. The secondary structure of the core domain is a typical HAD-superfamily Rossmannoid fold with a six-stranded parallel β-sheet (β1–β6) surrounded by four α-helices (α5–α8) and three 3_{10}-helices. β-Strand 3 and α-helix 6 are connected by one 3_{10}-helix, and two additional 3_{10}-helices are found between β-strand 2 and β-strand 3. There is a longer loop (loop III; residues 199–214) between the last two β-strands (β5 and β6).

The subdomain includes residues 15–102 and represents approximately 38% of the amino-acid residues. Its secondary structure consists of a four-helix bundle, and a 3_{10}-helix connects α-helix 2 and α-helix 3. Helices α1 and α2 are oriented approximately vertically, and α1 and α4, which mark the start and end of the subdomain, are inserted into the core domain between β1 and α5. The hinge area between the core domain and the subdomain consists of loop I (residues 8–14) and loop II (residues 102–110). Loop I has the appearance of a highly twisted letter N (Fig. 1*a*).

Located in a cavity between the core domain and the subdomain there is a cluster with strong electron density that we assumed was a metal atom. As no metal atoms were added during protein purification and as we used 1 m*M* EDTA when performing the overnight cleavage of the GST tag, we presume that this must be an Mg^{2+} atom that bound to ps-2-HAD during the crystallization procedure, as the crystallization reagent contained 200 m*M* $MgCl_2$. This metal ion is octahedrally coordinated by monodentate carboxylates from the side chains of Asp8 and Asp180, the main-chain O atom of Asp10 and three water molecules, which is in agreement with the coordination geometry of magnesium (Fig. 1*b*).

In the crystal structure of ps-2-HAD the two molecules in the asymmetric unit can be superimposed almost completely. Structural comparison of molecules *A* and *B* with *CCP4mg* (McNicholas *et al.*, 2011) yields an r.m.s.d. of 0.26 Å. The two molecules interact with each other *via* two hydrogen bonds between Gln44 and Arg50 from the α2 helices of each molecule, which are packed as antiparallel helices (Figs. 1*c* and 1*d*).

3.2. Ps-2-HAD catalyses the dehalogenation of both D- and L-substrates

D-CPA and L-CPA were used to test the catalytic capacity of ps-2-HAD for substrates with different chirality using the phenol red method described by Littlechild *et al.* (2009). The results showed that ps-2-HAD is active towards both D- and

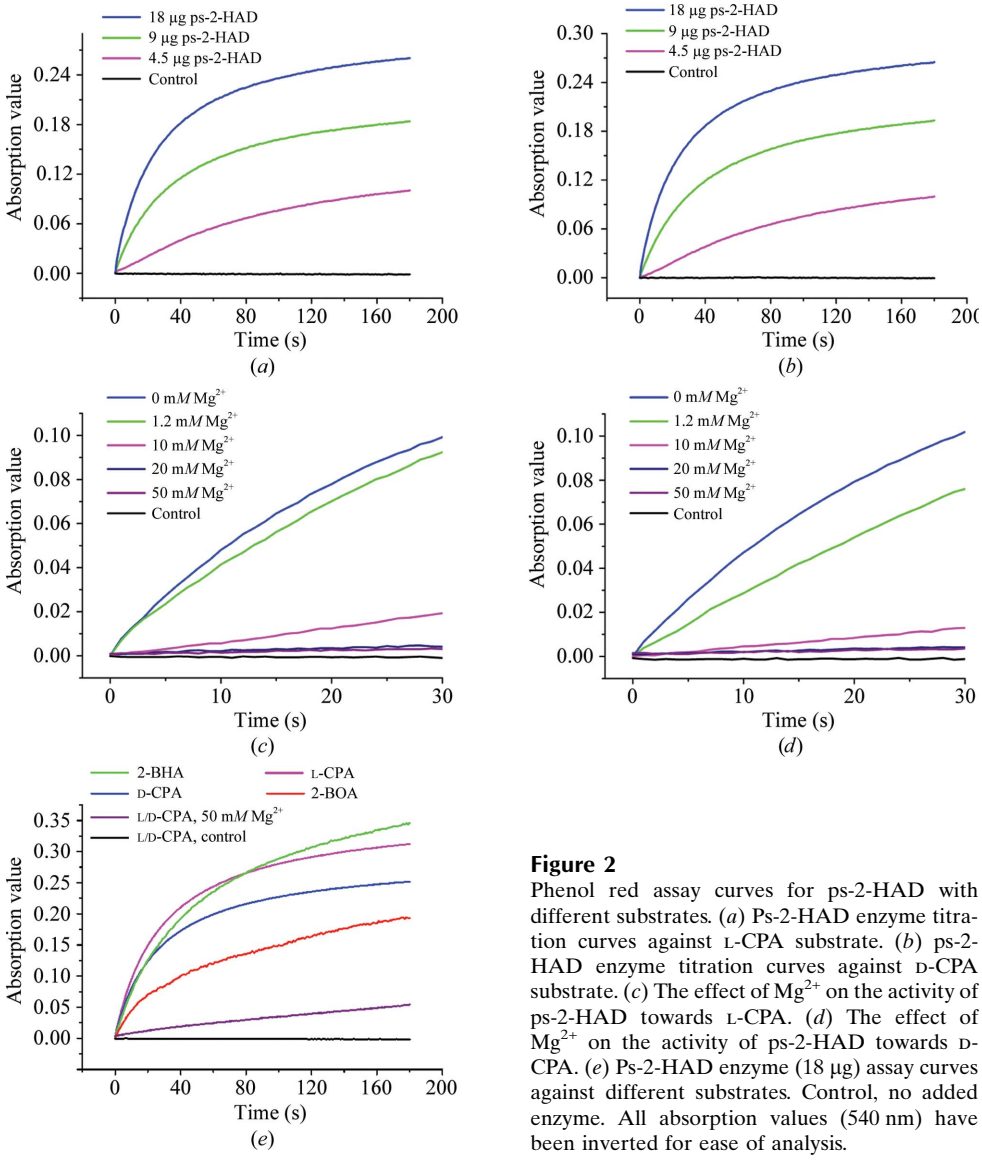

Figure 2
Phenol red assay curves for ps-2-HAD with different substrates. (*a*) Ps-2-HAD enzyme titration curves against L-CPA substrate. (*b*) ps-2-HAD enzyme titration curves against D-CPA substrate. (*c*) The effect of Mg^{2+} on the activity of ps-2-HAD towards L-CPA. (*d*) The effect of Mg^{2+} on the activity of ps-2-HAD towards D-CPA. (*e*) Ps-2-HAD enzyme (18 µg) assay curves against different substrates. Control, no added enzyme. All absorption values (540 nm) have been inverted for ease of analysis.

L-substrates (Fig. 2). The DL-catalytic activity of ps-2-HAD was further confirmed using mercuric thiocyanate (Iwasaki, Kokubu *et al.*, 1956; Supplementary Fig. S1[1]). The rate of catalytic reaction towards both D-CPA and L-CPA increased markedly as the amount of enzyme in the reaction solution increased (Figs. 2*a* and 2*b*). A greater amount of enzyme was required in the method involving mercuric thiocyanate, possibly because this method is much less sensitive than the phenol red method for measuring ps-2-HAD activity.

Since all 2-HADs with known structures do not bind magnesium, we wondered whether the magnesium ion plays a functional role in the structure; we therefore tested the enzymatic activity of ps-2-HAD with different concentrations of magnesium. Magnesium had an inhibitory effect on ps-2-HAD activity; the enzymatic activity decreased gradually with increasing concentrations of magnesium (Figs. 2*c* and 2*d*). Activity was abolished when the magnesium concentration reached about 20 m*M*. These results suggest that either the magnesium-binding cavity at least partially overlaps with the active site of ps-2-HAD or the coordinated residues or water molecules are involved directly in the catalytic reaction.

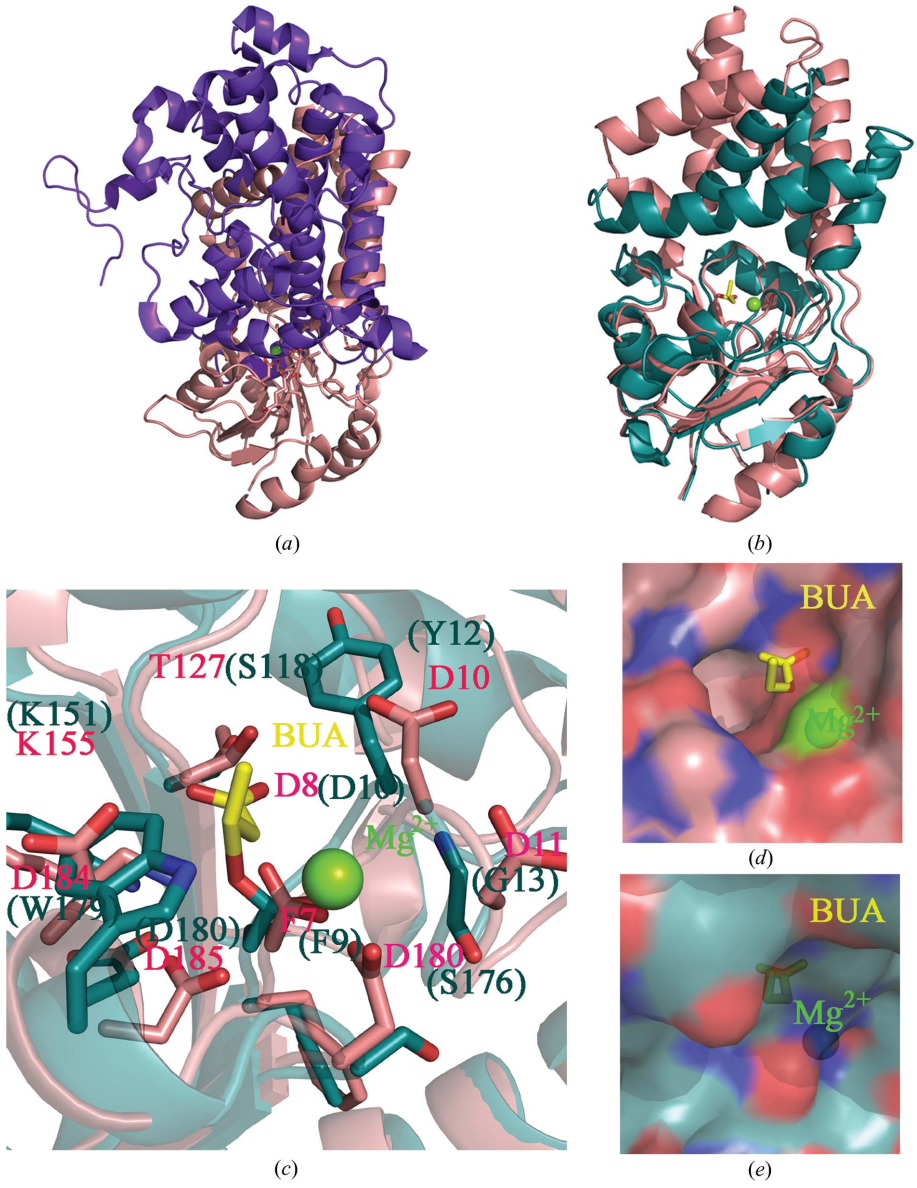

Figure 3
(*a*) Structural comparison of ps-2-HAD and DehI (PDB entry 3bjx; Schmidberger *et al.*, 2008). Ps-2-HAD is coloured salmon and DehI is coloured purple. The magnesium ion in ps-2-HAD is shown as a green ball. (*b*) Structural comparison of ps-2-HAD and L-DEX YL (PDB entry 1zrm). Ps-2-HAD is coloured salmon and L-DEX YL is coloured deep teal. The magnesium in ps-2-HAD is shown as a green ball. The product BUA in L-DEX YL is shown in stick representation, with C atoms coloured yellow and O atoms coloured red. (*c*) Superposition of the potential active site of ps-2-HAD on the active site of L-DEX YL. Adjacent residues are shown in stick representation. L-2-Chlorobutyrate forms an ester bond with Asp10 in L-DEX YL. The colour code is the same as in (*b*). (*d*, *e*) Surface representation of ps-2-HAD (*d*) and L-DEX YL (*e*) indicating that ps-2-HAD has a deeper and wider active site compared with L-DEX YL. The colour code is the same as in (*b*).

3.3. Structural comparisons imply that ps-2-HAD has an active site at a similar position to other L-2-HADs

Although ps-2-HAD can catalyse the dehalogenation of both D- and L-substrates, it only shows 5% sequence identity to DehI, the only DL-HAD of known structure (Supplementary Fig. S2*a*). Their structures are quite different and have no overlap (Fig. 3*a*). Interestingly, ps-2-HAD shares about 20% sequence homology with L-2-HADs, and the most conserved Asp residue in the L-2-HADs is also conserved in ps-2-HAD (Supplementary Fig. S2*b*). Superposition of ps-2-HAD with four previously reported L-2-HAD structures showed that they have a similar overall structure. As the known L-2-HAD structures are very similar, we selected the best characterized structure, L-DEX YL, for a detailed comparison with ps-2-HAD. Superposition of the two structures showed that their core domains can be overlapped completely, with the two structures differing in the orientation of the subdomains (Fig. 3*b*). The two structures had an r.m.s.d. of 2.4 Å over 166 C^{α} atoms as calculated by *CCP4mg* (McNicholas *et al.*, 2011).

The active site of L-HADs is located in the pocket between the core domain and the subdomain. In the reported crystal

[1] Supplementary material has been deposited in the IUCr electronic archive (Reference: XB5068). Services for accessing this material are described at the back of the journal.

structures of L-DEX YL in complex with monochloroacetate (ACY; PDB entry 1zrn) or L-2-chlorobutyrate (BUA; PDB entry 1zrm), the nucleophile Asp10 covalently binds to the dechlorinated moiety of the substrate to form an ester intermediate in the active site. In our structure, the Asp8 residue of ps-2-HAD can be superimposed perfectly with the Asp10 residue in L-DEX YL. The Thr127 residue of ps-2-HAD corresponds to and can be superimposed with Ser118 from L-DEX YL, which forms a hydrogen bond to the carboxyl-terminus of the substrate (Esaki *et al.*, 1998; Fig. 3*c*). Some other crucial conserved residues such as Phe7 (Phe9 in L-DEX YL) and Lys155 (Lys151 in L-DEX YL) are also almost identical in the two structures (Fig. 3*c*). However, some other amino-acid residues, such as Tyr12, Gln42, Leu45, Asn177 and Trp179 in L-DEX YL, which form a hydrophobic pocket stabilizing the alkyl groups of the substrate molecules, differ somewhat between the two structures. These results indicate that ps-2-HAD may have an active site located in a similar position to that of the L-2-HADs. Magnesium is bound at the presumed active site of ps-2-HAD (Fig. 3*c*), possibly explaining the inhibitory effect of magnesium.

3.4. Ps-2-HAD has a more open substrate-binding pocket

Previous reports from other groups have shown that DhlB can only accommodate small substrates of up to three C atoms in size (such as chloropropionic acid; van der Ploeg *et al.*, 1991), that L-haloacid dehalogenase from the thermophilic archaeon *S. tokodaii* can act on 2-chlorobutyric acid (Littlechild *et al.*, 2009) and that L-DEX YL can catalyze the dehalogenation of substrates with longer chain lengths such as 2-chloro-*n*-caproate in aqueous solution but with very low activity compared with shorter substrates such as L-2-chloropropionic acid (Liu *et al.*, 1994). Among the three enzymes referred to above, DhlB has the most enclosed active site while L-DEX YL has the most exposed active site; this is consistent with their activity towards substrates of various sizes.

Superposition of ps-2-HAD with other L-HAD structures shows that the presumed active-site cavity of ps-2-HAD is wider and more open to solvent than that of L-DEX YL (Fig. 3*d*) owing to the different orientations of the subdomains in these structures, thus suggesting that ps-2-HAD may catalyze the dehalogenation of substrates with longer carbon chains. To confirm this, 2-bromohexanoic acid (2-BHA) and 2-bromooctanoic acid (2-BOA) were used to test the catalytic capacity of ps-2-HAD towards substrates with different carbon chain lengths using the phenol red method (Iwasaki, Utsumi *et al.*, 1956). The assay results showed that ps-2-HAD can catalyse the dehalogenation of substrates with at least eight C atoms (2-BOA) in aqueous solution (it was not possible to test longer carbon-chain substrates as they were not readily available commercially) and can thus catalyse the dehalogenation of substrates which are much longer than those of other HADs (which commonly act on substrates with three C atoms such as 2-CPA; Fig. 2*e*). Our results thus suggest that ps-2-HADs have a broader substrate specificity than other HADs.

3.5. The potential active site of ps-2-HAD

Structural comparison suggests that the active site of ps-2-HAD may be in a similar position to that in L-2-HADs, as the Asp8 residue of ps-2-HAD can be superimposed perfectly on the Asp10 residue of L-DEX YL. Since Asp10 is crucial for the activity of L-DEX YL and is very highly conserved in L-2-HADs, we questioned whether or not ps-2-HAD shares a common reaction mechanism with L-2-HADs and which residue is most important for ps-2-HAD activity.

To elucidate the reaction mechanism of ps-2-HAD, we designed eight mutants in which conserved or polar amino-acid residues near the presumed active site (including the six Asp residues Asp8, Asp10, Asp11, Asp180, Asp184 and Asp185, Thr127 and Lys155) were replaced by Ala; however, we were only able to purify four of these mutants (D8A,

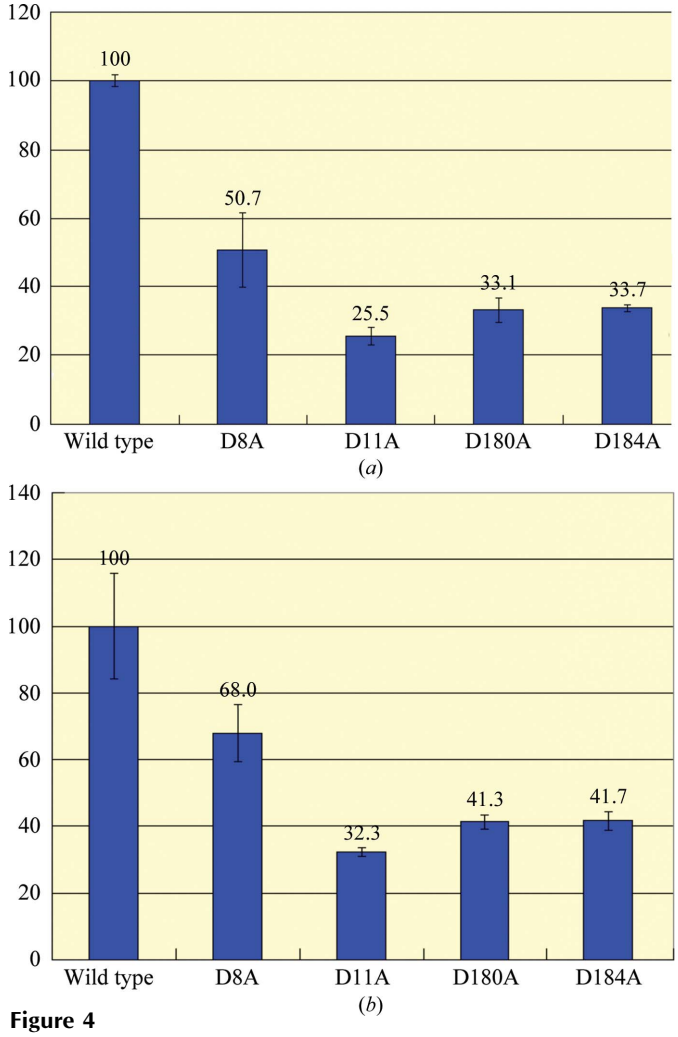

Figure 4
Enzymatic activity analysis of wild-type and mutant ps-2-HAD. The activity of wild-type ps-2-HAD was considered to be 100% and the activities of mutant proteins were expressed as a percentage of the wild-type control activity. (*a*) L-CPA was used as the substrate for enzyme assay of the wild-type and mutant proteins. (*b*) D-CPA was used as the substrate for enzyme assay of wild-type and mutant proteins.

D11A, D180A and D184A) successfully. Each of the four mutants was tested for enzymatic activity (Fig. 4). Unexpectedly, the D8A mutant retained about half the enzyme activity of the wild type, indicating that the conserved Asp is not essential for ps-2-HAD activity. We hypothesize that although ps-2-HAD has an active site located at a similar position to that in other L-HADs, it may function in a different way.

The activity of the other three mutants was less than half that of the wild type, with the D11A mutant having the lowest activity (Fig. 4). With the exception of Asp8, all of the other residues are not conserved among the HADs. These results further strengthen our hypothesis that ps-2-HAD has a novel catalytic mechanism. No single amino-acid residue in these mutants appears to be vital for ps-2-HAD activity. Since some of the mutants that we designed (*e.g.* D10A and D185A) could not be expressed successfully, it is possible that one of these residues may play a fundamental role in the catalytic reaction.

4. Conclusions

Structure-superposition and mutagenesis experiments imply that the reaction mechanism of ps-2-HAD differs somewhat from those of both L-2-HADs and DL-2-HADs. However, previous results showed that an Asp residue, either Asp10 in L-DEX YL (an L-2-HAD) or Asp194 in DL-DEX 113 (a DL-2-HAD), is required for catalytic activity (Liu *et al.*, 1997; Kurihara *et al.*, 1995). Ps-2-HAD has a unique structural feature in that there are as many as six Asp residues near the presumed active site; it is possible that these Asp residues cooperate to fulfill the catalytic function (Fig. 3*c*). This would explain why single mutations of these Asp residues reduce but do not abolish enzymatic activity. The inhibitory effect of magnesium is likely to be explained by our hypothesis that magnesium binds competitively to one or more substrate-interacting residues (such as Asp8 and Asp180) or water molecules, leading to disruption of the substrate-binding pocket. Taken together, our observations suggest that the active site and the catalytic action of ps-2-HAD are evidently different from those of either DL-2-HADs or L-2-HADs and provide a structural framework for further detailed investigation of its catalytic process.

We are grateful to the faculty of the Shanghai Synchrotron Radiation Facility for their help in data collection. This work was supported by grants from the Major State Basic Research Development Program of China (973 Program; grant No. 2011CBA00902) and the National Natural Science Foundation of China (grant No. 31021062).

References

Adams, P. D. *et al.* (2010). *Acta Cryst.* D**66**, 213–221.
Corpet, F. (1988). *Nucleic Acids Res.* **16**, 10881–10890.
Emsley, P. & Cowtan, K. (2004). *Acta Cryst.* D**60**, 2126–2132.
Esaki, N., Li, Y.-F., Hata, Y., Fujii, T., Hisano, T., Nishihara, M. & Kurihara, T. (1998). *J. Biol. Chem.* **273**, 15035–15044.
Esaki, N., Nardi-Dei, V., Kurihara, T., Park, C., Miyagi, M., Tsunasawa, S. & Soda, K. (1999). *J. Biol. Chem.* **274**, 20977–20981.
Gouet, P., Courcelle, E., Stuart, D. I. & Métoz, F. (1999). *Bioinformatics*, **15**, 305–308.
Hisano, T., Hata, Y., Fujii, T., Liu, J. Q., Kurihara, T., Esaki, N. & Soda, K. (1996). *J. Biol. Chem.* **271**, 20322–20330.
Iwasaki, I., Kokubu, N. & Katsura, T. (1956). *Bull. Chem. Soc. Jpn*, **29**, 379–387.
Iwasaki, I., Utsumi, S., Hagino, K. & Ozawa, T. (1956). *Bull. Chem. Soc. Jpn*, **29**, 860–864.
Kurihara, T., Liu, J.-Q., Nardi-Dei, V., Koshikawa, H., Esaki, N. & Soda, K. (1995). *J. Biochem.* **117**, 1317–1322.
Laskowski, R. A., MacArthur, M. W., Moss, D. S. & Thornton, J. M. (1993). *J. Appl. Cryst.* **26**, 283–291.
Li, Y.-F., Hata, Y., Fujii, T., Hisano, T., Nishihara, M., Kurihara, T. & Esaki, N. (1998). *J. Biol. Chem.* **273**, 1503–15044.
Littlechild, J. A., Rye, C. A., Isupov, M. N. & Lebedev, A. A. (2009). *Extremophiles*, **13**, 179–190.
Liu, J.-Q., Kurihara, T., Hasan, A. K. M. Q., Nardidei, V., Koshikawa, H., Esaki, N. & Soda, K. (1994). *Appl. Environ. Microbiol.* **60**, 2389–2393.
Liu, J.-Q., Kurihara, T., Miyagi, M., Tsunasawa, S., Nishihara, M., Esaki, N. & Soda, K. (1997). *J. Biol. Chem.* **272**, 3363–3368.
McNicholas, S., Potterton, E., Wilson, K. S. & Noble, M. E. M. (2011). *Acta Cryst.* D**67**, 386–394.
Nardi-Dei, V., Kurihara, T., Park, C., Esaki, N. & Soda, K. (1997). *J. Bacteriol.* **179**, 4232–4238.
Otwinowski, Z. & Minor, W. (1997). *Methods Enzymol.* **276**, 307–326.
Ploeg, J. van der, van Hall, G. & Janssen, D. B. (1991). *J. Bacteriol.* **173**, 7925–7933.
Ridder, I. S., Rozeboom, H. J., Kalk, K. H. & Dijkstra, B. W. (1999). *J. Biol. Chem.* **274**, 30672–30678.
Ridder, I. S., Rozeboom, H. J., Kalk, K. H., Janssen, D. B. & Dijkstra, B. W. (1997). *J. Biol. Chem.* **272**, 33015–33022.
Schmidberger, J. W., Wilce, J. A., Tsang, J. S. H. & Wilce, M. C. J. (2007). *J. Mol. Biol.* **368**, 706–717.
Schmidberger, J. W., Wilce, J. A., Weightman, A. J., Whisstock, J. C. & Wilce, M. C. J. (2008). *J. Mol. Biol.* **378**, 284–294.
Terwilliger, T. C. (2000). *Acta Cryst.* D**56**, 965–972.
Winn, M. D. *et al.* (2011). *Acta Cryst.* D**67**, 235–242.